

Steel–Concrete Composite Beams Considering Shear Slip Effects

Jianguo Nie¹ and C. S. Cai, P.E., M.ASCE²

Abstract: The present study investigated the effects of shear slip on the deformation of steel–concrete composite beams. The equivalent rigidity of composite beams considering three different loading types was first derived based on equilibrium and curvature compatibility, from which a general formula to account for slip effects was then developed. The predicted results were compared with measurements of six specimens tested in the present study and other available test results for both simply supported and continuous beams. It was found that including slip effects has significantly improved the accuracy of prediction. For typical beams used in practice, shear slip in partial composite beams has a significant contribution to beam deformation. Even for full composite beams, slip effects may result in stiffness reduction up to 17% for short span beams. However, slip effects are ignored in many design specifications that use transformed section method except that American Institute of Steel Construction (AISC) specifications recommend a calculation procedure in the commentary. In the AISC procedure, stress and deflection calculations of partially composite girders are based on effective section modulus and moment of inertia to account for slip, while ignoring slip effects in full composite sections. For full composite sections, the effective section modulus and moment of inertia calculated with the AISC specifications are larger than that of present study, meaning that the specifications are not on the conservative side. For partial composite sections, the AISC predictions are more conservative than the present study.

DOI: 10.1061/(ASCE)0733-9445(2003)129:4(495)

CE Database subject headings: Composite beams; Slip; Deformation.

Introduction

Taking advantage of the high tensile strength of steel materials and high compressive strength of concrete materials, composite steel construction has gained in popularity during the past decades. With the development of high-performance steels (HPSs) and high-performance concrete (HPC), composite steel bridges have been designed to span lengths greater than were previously impossible with ordinary materials, while reducing the cost of composite bridges by as much as 10%. This gain, however, could be negated by deflection controlling the design, rather than strength. Therefore, particular attention has to be paid to the deflection calculation of modern and future composite structures.

The composite action between steel and concrete depends on the performance of shear connectors at their interface. The use of HPS and HPC requires more shear connectors for full composite action. Due to the limitation of the number of shear connectors that the top flange can accommodate or for an optimal design, a partial composite design may be selected. A partial composite design will result in more shear deformation (slip) at the steel–concrete interface, which, eventually, leads to an additional de-

flexion. Even for a full composite design, deflection calculations ignoring this interface slip will underestimate deflections compared with experimental measurements (Johnson 1975). At service load, the actual stiffness of beams with full composite design is about 85–90% of their calculated stiffness where slip is ignored (McGarraugh and Baldwin 1971). The loss in stiffness can be attributed to the fact that the shear connectors are flexible, permitting some slip or loss of interaction between the concrete slab and steel beam, even though their strength is sufficient for full composite action (Grant et al. 1977).

In current design practice, a bridge structural system consisting of steel beams and concrete slab is usually simplified as a combination of individual composite girders on which the bridge analysis and design are conducted. Each composite girder consists of a steel beam and a portion of concrete slab, effective slab width, connected with shear connectors. In the American Association of State Highway and Transportation Officials (AASHTO) (AASHTO 1998) specifications, no guidelines are provided in calculating the slip-induced deflection. While American Institute of Steel and Concrete (AISC 1993) specifies a reduced effective moment of inertia to account for slip in partial composite sections, no reduction is applied to full-composite sections. To preserve the benefits using high-performance materials, the accuracy of these design specifications should be re-examined.

With the development of computational tools and computers, engineers now commonly use more complicated analysis such as finite element models to analyze the entire structural systems (Manfredi et al. 1999; Sebastian and McConnel 2000). To investigate the effects of the shear transfer characteristics between concrete and steel, the actual shear stiffness of the studs and the friction/bond at the interface can be modeled. One way to model the stud stiffness is to use spring elements (Dezi et al. 2001). The

¹Professor, Dept. of Civil Engineering, Tsinghua Univ., Beijing 100084, China.

²Assistant Professor, Dept. of Civil and Environmental Engineering, Louisiana State Univ., 3502 CEBA, Baton Rouge, LA 70803.

Note. Associate Editor: Mark D. Bowman. Discussion open until September 1, 2003. Separate discussions must be submitted for individual papers. To extend the closing date by one month, a written request must be filed with the ASCE Managing Editor. The manuscript for this paper was submitted for review and possible publication on September 27, 2001; approved on June 28, 2002. This paper is part of the *Journal of Structural Engineering*, Vol. 129, No. 4, April 1, 2003. ©ASCE, ISSN 0733-9445/2003/4-495–506/\$18.00.

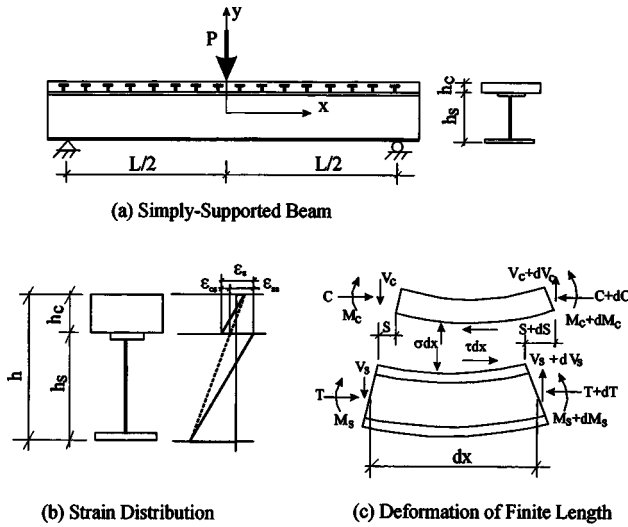


Fig. 1. Calculation model for simply supported beam

deformation characteristics can be assigned to these spring elements in both vertical and horizontal (interface shear) directions. The individual studs can also be modeled as beam elements that will give the shear force of each individual stud. Such analysis will predict more accurate deflection but is not suitable for routine design office use.

The main objective of this research is to develop calculation tools for the deflection of composite steel members considering the effect of interface slip. The recommended procedure is suitable for design office use and is in line with the current code specifications. While the present study focuses on the regular steel and concrete composite beams, the procedure is equally valid for HPS and HPC composite beams whose deflection predictions are critical issues.

Prediction of Interface Slip

For deflection calculation under service load, steel–concrete composite structures are usually modeled elastically since the steel is in the elastic range and concrete experiences low stress levels. Elastic analysis is thus used in the present study and it is assumed that: (1) the shear stress at the interface is proportional to the slip; (2) steel girder and concrete flange have the same curvature; and (3) for simplicity, the section is symmetric about its vertical axis.

The assumption (1) gives

$$p\tau = KS \quad (1)$$

where p = longitudinal spacing (pitch) of shear studs; τ = shear stress; K = shear stiffness of shear stud; and S = slip between steel and concrete.

For a simply supported beam shown in Fig. 1, equilibrium of the finite length dx in the horizontal direction gives

$$\frac{dC}{dx} = \frac{dT}{dx} = -\tau \quad (2)$$

where C = compression in concrete; and T = tension in steel.

Equilibrium in the vertical direction gives

$$V_c + V_s = \frac{P}{2} \quad (3)$$

where V_c = shear force carried by concrete; V_s = shear force carried by steel; and P = total load at the mid span.

The moment equilibrium of the concrete and steel segments gives

$$\frac{dM_c}{dx} = -V_c + \frac{\tau y_{cb}}{2} - \sigma dx \quad (4)$$

$$\frac{dM_s}{dx} = -V_s + \frac{\tau y_{st}}{2} + \sigma dx \quad (5)$$

where M_c = moment carried by concrete; M_s = moment carried by steel; σ = normal stress between steel and concrete interface; y_{cb} = distance from bottom of concrete to its neutral axis; and y_{st} = distance from top of steel to its neutral axis.

Curvature compatibility between the concrete and steel gives the curvature ϕ as

$$\phi = \frac{M_s}{E_s I_s} = \frac{M_c}{E_c I_c} \quad (6)$$

where E_s = elastic modulus of steel; I_s = moment inertia of steel; E_c = elastic modulus of concrete; and I_c = moment inertia of concrete.

Solving Eqs. (2)–(6) yields

$$\frac{d\phi}{dx} = \frac{-0.5P + \tau d_c}{E_s I_s + E_c I_c} \quad (7)$$

where $d_c = y_{cb} + y_{st}$.

Strains at the bottom of concrete (ϵ_{cb}) and top of steel (ϵ_{st}) are calculated from the moment and axial force as

$$\epsilon_{cb} = \frac{M_c y_{cb}}{E_c I_c} - \frac{C}{E_c A_c} = \phi y_{cb} - \frac{C}{E_c A_c} \quad (8)$$

$$\epsilon_{st} = -\frac{M_s y_{st}}{E_s I_s} + \frac{T}{E_s A_s} = -\phi y_{st} + \frac{T}{E_s A_s} \quad (9)$$

where A_c = area of concrete; and A_s = area of steel.

The relative slip strain at the interface is calculated as

$$\frac{ds}{dx} = \epsilon_s = \epsilon_{cb} - \epsilon_{st} = \phi d_c - \frac{T}{E_s A_s} - \frac{C}{E_c A_c} \quad (10)$$

Derivating with respect to x in Eq. (10) and then using Eqs. (1), (2), and (7) gives the differential equation as

$$\frac{d^2 S}{dx^2} = \alpha^2 S - \frac{\alpha^2 \beta P}{2} \quad (11)$$

where $\alpha^2 = K/(A_1 E_s I_0 p)$; $\beta = A_1 d_c p/K$; $A_1 = A_0/(I_0 + A_0 d_c^2)$; $A_0 = (A_s A_c)/(n A_s + A_c)$; $I_0 = I_c/n + I_s$; and $n = E_s/E_c$.

Solving Eq. (11) and using the boundary conditions that $S = 0$ at $x = 0$, and $dS/dx = 0$ at $x = L/2$ (where L = span length) gives the slip solution for $0 \leq x \leq L/2$ as

$$S = \frac{\beta P (1 + e^{-\alpha L} - e^{\alpha x - \alpha L} - e^{-\alpha x})}{2(1 + e^{-\alpha L})} \quad (12)$$

Correspondingly, slip strain solution is

$$\epsilon_s = \frac{\alpha \beta P (e^{-\alpha x} - e^{\alpha x - \alpha L})}{2(1 + e^{-\alpha L})} \quad (13)$$

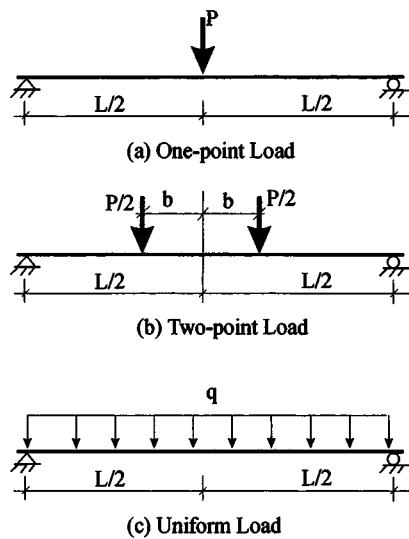


Fig. 2. Load definitions

Effect of Slip on Section Rigidity

The additional curvature due to slip is calculated as

$$\Delta\phi = \frac{\epsilon_{cs}}{h_c} = \frac{\epsilon_{ss}}{h_s} = \frac{\epsilon_s}{h} \quad (14)$$

where h_c =depth of concrete; h_s =depth of steel; and h =depth of entire section.

For the case of simply supported beams with a single load shown in Fig. 2(a), the additional deflection due to slip is then calculated from the curvature as

$$\Delta f_1 = \beta P \left(\frac{L}{4h} + \frac{1 - \alpha L}{2\alpha h(1 + e^{\alpha L})} \right) \quad (15)$$

Similarly, for two-point load (total load= P) and uniform load q shown in Figs. 2(b) and (c), the additional deflections due to slip are derived, respectively, as

$$\Delta f_2 = \beta P \left(\frac{L - 2b}{4h} + \frac{e^{\alpha b} - e^{\alpha(L-b)}}{2\alpha h(1 + e^{\alpha L})} \right) \quad (16)$$

$$\Delta f_3 = \beta q \left(\frac{L^2}{8h} + \frac{2e^{(\alpha L)/2} - 1 - e^{\alpha L}}{\alpha^2 h(1 + e^{\alpha L})} \right) \quad (17)$$

where Δf_2 =additional deflection due to slip for two-point load; Δf_3 =additional deflection due to slip for uniform load; and b =distance between loading point and the mid span.

Considering the fact that $e^{-\alpha L}$ is close to zero since αL is larger than 4 for typical girders as will be discussed later, Δf_1 , Δf_2 , and Δf_3 in Eqs. (15)–(17) can be simplified as

$$\Delta f_1 = \beta P \left(\frac{L}{4h} - \frac{1}{2\alpha h} \right) \quad (18)$$

$$\Delta f_2 = \beta P \left(\frac{L - 2b}{4h} - \frac{e^{-\alpha b}}{2\alpha h} \right) \quad (19)$$

$$\Delta f_3 = \beta q \left(\frac{L^2}{8h} - \frac{2}{\alpha^2 h} \right) \quad (20)$$

The total deflection calculated from elastic deformation and slip-induced deflection is

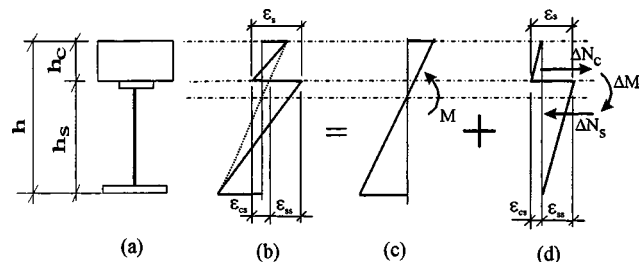


Fig. 3. Calculation model for additional moment

$$f_1 = f_{e1} + \Delta f_1 = \frac{PL^3}{48EI} + \beta P \left(\frac{L}{4h} - \frac{1}{2\alpha h} \right) \quad (21)$$

$$f_2 = f_{e2} + \Delta f_2 = \frac{P}{12EI} \left[2 \left(\frac{L}{2} - b \right)^3 + 3b \left(\frac{L}{2} - b \right) (L - b) \right] + \beta P \left(\frac{L - 2b}{4h} - \frac{e^{-\alpha b}}{2\alpha h} \right) \quad (22)$$

$$f_3 = f_{e3} + \Delta f_3 = \frac{5qL^4}{384EI} + \beta q \left(\frac{L^2}{8h} - \frac{2}{\alpha^2 h} \right) \quad (23)$$

where EI =section rigidity based on transformed section.

The above deflections can be written in terms of effective rigidity B in a format similar to one without slip as

$$f_1 = \frac{PL^3}{48B_1} \quad (24)$$

$$f_2 = \frac{P}{12B_2} \left[2 \left(\frac{L}{2} - b \right)^3 + 3b \left(\frac{L}{2} - b \right) (L - b) \right] \quad (25)$$

$$f_3 = \frac{5qL^4}{384B_3} \quad (26)$$

where

$$B_i = \frac{EI}{1 + \xi_i} \quad (27)$$

$$\xi_1 = \eta \left(\frac{1}{2} - \frac{1}{\alpha L} \right) \quad (28)$$

$$\xi_2 = \eta \left[\frac{0.5 - b/L - e^{-\alpha L(b/L)}/(\alpha L)}{4(2(0.5 - b/L)^3 + 3(0.5 - b/L)(1 - b/L)b/L)} \right] \quad (29)$$

$$\xi_3 = \eta \left(\frac{1}{2} - \frac{4}{(\alpha L)^2} \right) / 1.25 \quad (30)$$

where $\eta = 24EI\beta/(L^2h)$; and $EI = E_s(I_0 + A_0d_c^2) = E_sA_0/A_1$ =rigidity of transformed section.

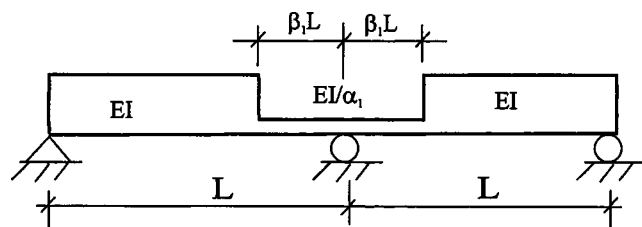


Fig. 4. Calculation model for continuous beam

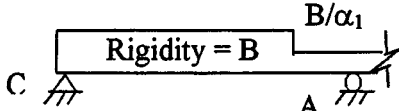
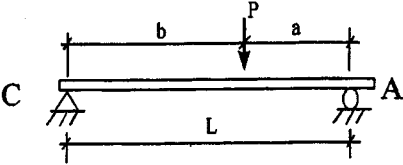
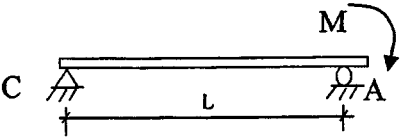
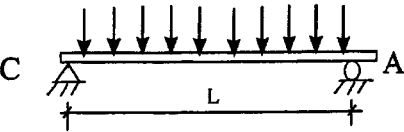
	
	$f = \frac{PL^3}{48B} \left[\frac{3a}{L} - \frac{4a^3}{L^3} + \frac{8b\beta_1^3}{L}(\alpha_1 - 1) \right] \quad \beta_1 L \leq a \leq \frac{L}{2}$ $f = \frac{PL^3}{48B} \left[\frac{3a}{L} - \frac{4\alpha_1 a^3}{L^3} - \frac{4\beta_1^2(2\beta_1 - 3)a}{L}(\alpha_1 - 1) \right] \quad a \leq \beta_1 L$ $f = \frac{PL^3}{48B} \left[\frac{4ab^2}{L^3} + \frac{b}{L^2}(3a - b) + \frac{8b\beta_1^3}{L}(\alpha_1 - 1) \right] \quad a > \frac{L}{2}$ $\theta_A = \frac{PL^2}{6B} \left[\frac{ab^2}{L^3} + \frac{ab}{L^2} + \frac{b}{L}\beta_1^2(3 - 2\beta_1)(\alpha_1 - 1) \right] \quad a \geq \beta_1 L$ $\theta_C = \frac{PL^2}{6B} \left[\frac{a^2b}{L^3} + \frac{ab}{L^2} + \frac{2b}{L}\beta_1^3(\alpha_1 - 1) \right] \quad a \geq \beta_1 L$ $\theta_A = \frac{PL^2}{6B} \left[-\frac{a^2b\alpha_1}{L^3} - \frac{2a^2\alpha_1}{L^2} + \frac{2a(1 - \beta_1)^3}{L} + \frac{2a\alpha_1\beta_1(\beta_1^2 - 3\beta_1 + 3)}{L} \right] \quad a < \beta_1 L$ $\theta_C = \frac{PL^2}{6B} \left[-\frac{a^3\alpha_1}{L^3} + \frac{a(\beta_1 - 1)^2(2\beta_1 + 1)}{L} + \frac{a\alpha_1\beta_1^2(3 - 2\beta_1)}{L} \right] \quad a < \beta_1 L$
	$f = \frac{ML^2}{48B} \left[3 + 4\beta_1^2(3 - 2\beta_1)(\alpha_1 - 1) \right]$ $\theta_A = \frac{ML}{6B} \left[2(1 - \beta_1)^3 + 3\alpha_1\beta_1(1 - \beta_1)(2 - \beta_1) + \alpha_1\beta_1^2(3 - \beta_1) \right]$ $\theta_C = \frac{ML}{6B} \left[(1 - \beta_1)^2(1 + 2\beta_1) + \alpha_1\beta_1^2(3 - 2\beta_1) \right]$
	$f = \frac{qL^4}{384B} \left[5 + 8(4\beta_1^3 - 3\beta_1^4)(\alpha_1 - 1) \right]$ $\theta_A = \frac{qL^3}{24B} \left\{ \alpha_1 + (1 - \alpha_1) \left[4(1 - \beta_1)^3 - 3(1 - \beta_1)^4 \right] \right\}$ $\theta_C = \frac{qL^3}{24B} \left[1 + (4\beta_1^3 - 3\beta_1^4)(\alpha_1 - 1) \right]$

Fig. 5. Calculation formulas for side span considering slip effects

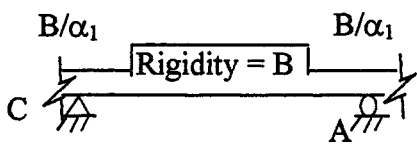
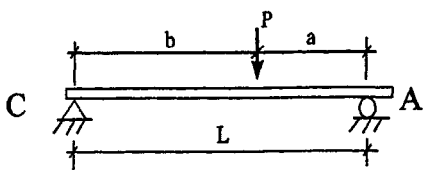
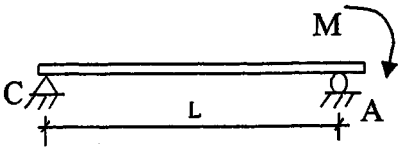
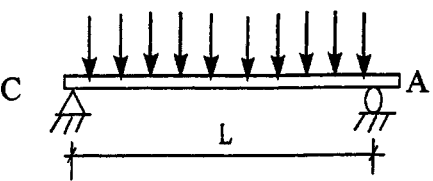
	
	$f = \frac{PL^3}{48B} \left[\frac{3ab}{L^2} + \frac{4ab^2}{L^3} - \frac{b^2}{L^2} + 8\beta_1^3(\alpha_1 - 1) \right]$ $\theta_A = \frac{PL}{6B} \left[\frac{ab}{L} \left(1 + \frac{b}{L} - \frac{b}{L}\beta_1 + 3\beta_1 \right) + \beta_1^3(3b - 2b\beta_1 + 2a\beta_1)(\alpha_1 - 1) \right]$ $\theta_C = \frac{PL}{6B} \left[\frac{ab}{L} \left(1 + \frac{a}{L} - \frac{a}{L}\beta_1 + 3\beta_1 \right) + \beta_1^3(3a - 2a\beta_1 + 2b\beta_1)(\alpha_1 - 1) \right]$
	$f = \frac{ML^2}{48B} \left[3 + 12\beta_1^2(\alpha_1 - 1) \right]$ $\theta_A = \frac{ML}{6B} \left[2 + 2\beta_1(3 - 3\beta_1 + \beta_1^2)(\alpha_1 - 1) \right]$ $\theta_C = \frac{ML}{6B} \left[1 + 2\beta_1^2(3\beta_1 - 2\beta_1^2)(\alpha_1 - 1) \right]$
	$f = \frac{qL^4}{384B} \left[5 + 16\beta_1^3(4 - 3\beta_1)(\alpha_1 - 1) \right]$ $\theta_A = \frac{qL^3}{24B} \left[1 + 2\beta_1^2(3 - 2\beta_1)(\alpha_1 - 1) \right]$ $\theta_C = -\theta_A$

Fig. 6. Calculation formulas for middle span considering slip effects

It can be seen from Eqs. (28) to (30) that the rigidity reduction factor is composed of two parts. The first part η is a function of beam geometrical parameters. The second part, denoted as $F = \xi_i/\eta$, is loading type dependent. It will be seen later that F is not very sensitive to load type. For this reason, and considering the fact that an actual beam usually carries different type of loading simultaneously, a formula similar to Eq. (30) is proposed for general loading as

$$\xi = \eta \left(0.4 - \frac{3}{(\alpha L)^2} \right) \quad (31)$$

The generalized equivalent or effective rigidity is

$$B = EI_{\text{eff}} = \frac{EI}{1 + \xi} \quad (32)$$

and the total deflection considering slip effect is

$$f = f_e(1 + \xi) \quad (33)$$

where f_e = elastic deflection based on transformed section.

Effect of Slip on Section Modulus

From Fig. 3, the slip-induced strain is linearly distributed across the section as

Table 1. Parameters of Specimens and Material Properties

Specimen	SCB-1	SCB-2	SCB-3	SCB-4	CCB-1	CCB-2
Width of concrete flange (mm)	500	800	800	800	800	800
Long. reinforcement <i>A</i>	7φ6	7φ6	12φ12	16φ12	6φ12	16φ12
Long. reinforcement <i>B</i>	7φ6	7φ6	7φ6	7φ6	7φ6	7φ6
Type of loading	two-point	two-point	one-point	one-point	one-point per span	one-point per span
Pitch of shear stud (mm)	115 (in shear span) 125 (in bending region)	115 (in shear span) 125 (in bending region)	148	148	148 (in outside region) 115 (in inside region)	148 (in outside region) 88 (in inside region)
Diameter of shear stud (mm)	19	19	19	19	19	19
Shear stud strength f_{su} (MPa)	431	431	431	431	431	431
Steel yield strength f_y (MPa)	310	310	310	310	310	310
Reinf. yield strength f_{ry} (MPa)	290	290	290	290	290	290
Concrete strength f_{cu} (MPa)	32	32	32	32	32	32

$$\epsilon_{ss} = \frac{h_s}{h} \epsilon_s \quad (34)$$

$$\Delta\phi = \frac{M\xi}{EI} = \frac{\epsilon_s}{h} \quad (38)$$

By using ϵ_{ss} for top flange and $0.5\epsilon_{ss}$ for web, the axial force variation in the steel section due to slip is

$$\Delta N_s = \frac{h_s}{h} E_s \epsilon_s (A_{ft} + 0.5A_w) \quad (35)$$

Correspondingly, the moment variation in the section is

$$\Delta M = \frac{h_s}{6h} E_s \epsilon_s (2h_c A_{ft} + hA_w) \quad (36)$$

where A_{ft} =area of top flange; and A_w =area of web.

Since the total curvature ϕ is related to the M (where M is the section bending moment without considering slip effect) as

$$\phi = \frac{M}{B} = \frac{M(1 + \xi)}{EI} \quad (37)$$

The slip-induced curvature is then interpreted from Eq. (37) as

from which we have

$$\epsilon_s = \frac{Mh\xi}{EI} \quad (39)$$

Considering Eqs. (36) and (39) gives

$$\Delta M = \frac{h_s E_s}{6EI} M \xi (2h_c A_{ft} + hA_w) \quad (40)$$

The internal moment (see Fig. 3) is then derived as

$$M_p = M - \Delta M = \left(1 - \frac{h_s E_s}{6EI} \xi (2h_c A_{ft} + hA_w) \right) M \quad (41)$$

where M =internal moment without slip; and M_p =internal moment including slip. When there is no slip, then $M_p = M$. The first yield moment M_{py} considering slip is related to the first yield moment M_y without slip as

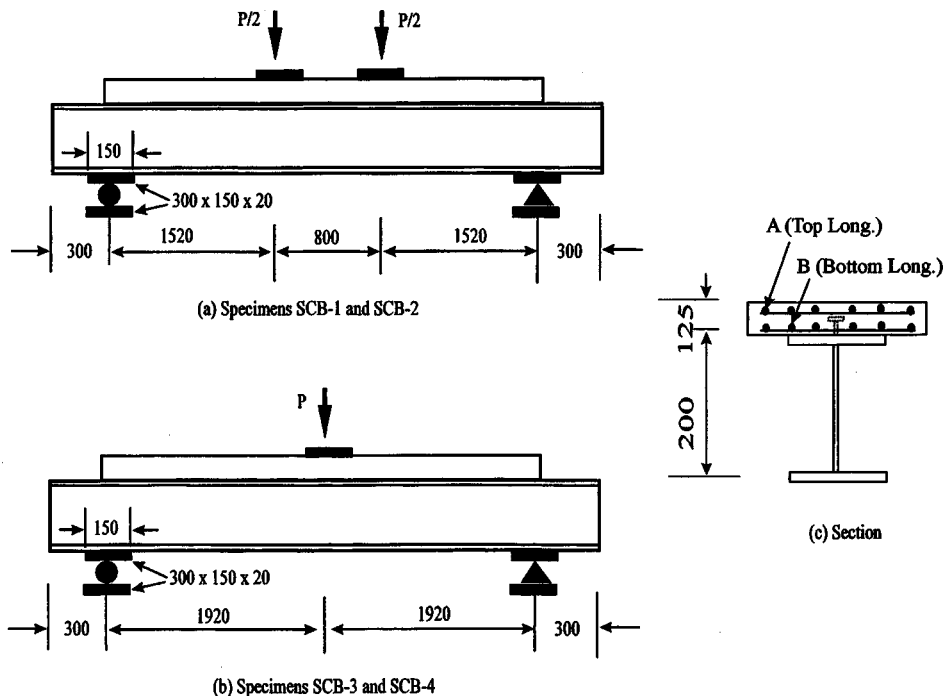


Fig. 7. Specimen dimension (mm) and loading

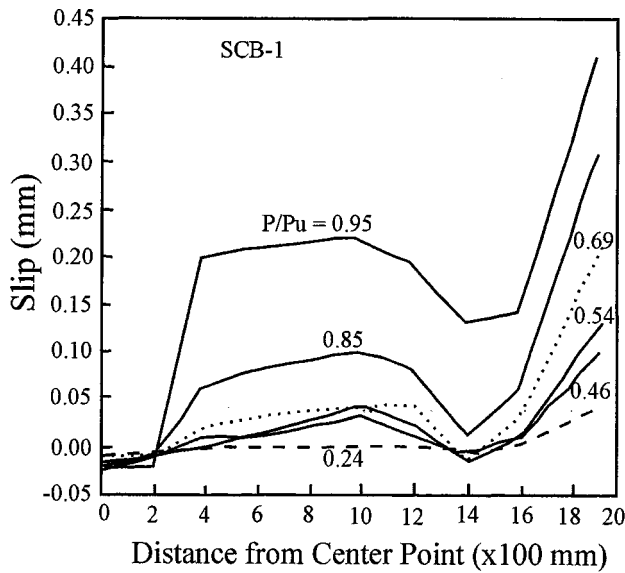


Fig. 8. Distribution of slip along span

$$M_{py} = \left(1 - \frac{h_s E_s}{6EI} \xi (2h_c A_{ft} + hA_w) \right) M_y \quad (42)$$

Since the slip effect reduces internal resistant moment by ΔM , the stress in the section actually increases due to the ΔM as

$$\sigma = \frac{M + \Delta M}{S_{tr}} = \left(1 + \frac{h_s E_s}{6EI} \xi (2h_c A_{ft} + hA_w) \right) \frac{M}{S_{tr}} \quad (43)$$

The effective section modulus is thus derived from Eq. (43) as

$$S_{eff} = \frac{S_{tr}}{\left(1 + \frac{h_s E_s}{6EI} \xi (2h_c A_{ft} + hA_w) \right)} \quad (44)$$

When considering slip effects, Eqs. (42), (43), and (44) show that the actual first yield moment reduces, the internal stress increases, and section modulus decreases, respectively, as compared with the case without slip.

Application to Continuous Beams

Many beams in building frames, platforms, and bridges are continuous structures. To increase the net clearances, the ratio of span length to depth is usually larger than 20. It is important to have reliable methods in predicting the deflection of these continuous structures. Traditionally, the variable section method shown in Fig. 4 is used. Specifically, only the reinforcement and steel materials are considered in the range of $\beta_1 L$ near each side of the supports and transformed section method is used in other areas. However, based on the comparison with experimental measurements of continuous beams that will be discussed later, the predicted deflection is less than the measured values. The writers believe that by including the slip effect, the accuracy of predicted deflection can be significantly improved.

The calculation can be done by dividing the continuous beam into a series of simply supported ones and using the principle of superposition to obtain the final results of the continuous beams. For each simply supported beam, the formulas developed earlier can be used to calculate the reduced rigidity B in each span. Then the deflections for different load cases can be calculated using the

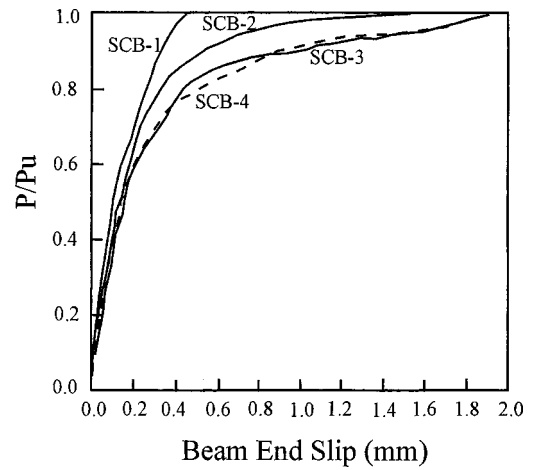


Fig. 9. Beam end slip versus load

formulas given in Figs. 5 and 6. The deflection of the continuous beam with variable section can also be predicted by other numerical approaches such as finite element analysis. The deflection is then modified by multiplying $(1 + \xi)$ to consider the slip effect.

Experimental Verification

Six specimens were tested in the experimental program. The parameters of these specimens are summarized in Table 1. As shown in Fig. 7, two-point loading was used for specimens SCB-1 and SCB-2; while one-point loading was used for specimens SCB-3 and SCB-4. Specimens CCB-1 and CCB-2 are two-span continuous beams with a span length of 3840 mm for each span. One concentrated load was applied at the center of each span.

The measured slip distributions under different loading along the span for a typical specimen (SCB-1) are shown in Fig. 8. The maximum slips were observed near the ends of beam. The curves of slips at beam end versus loading are shown in Fig. 9. It can be seen that the relationship between load and slip is fairly linear when P/P_u is less than 0.6, where P_u is the ultimate capacity. With the increase of loading, the relationship becomes highly nonlinear. It seems that the pitches of the shear studs have significant effects on the slip by comparing the measured slips of

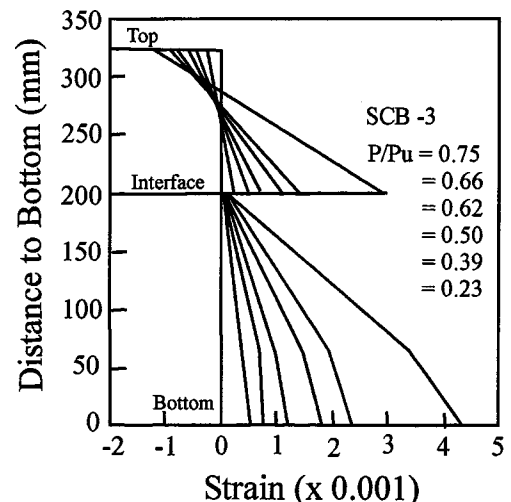


Fig. 10. Strain distribution across section

Table 2. Comparison of Deflection for Simply Supported Beams

Specimen source	Specimen	P/P_u	f_t (mm)	f_e (mm)	f_{acu} (mm)	f_{app} (mm)	f_e/f_t	f_{app}/f_t
Present study	SCB-1	0.69	13	9.6	12.2	12.1	0.74	0.93
	SCB-2	0.67	12.6	8.7	11.3	11.3	0.69	0.90
	SCB-3	0.57	9.1	6.9	9.4	9.2	0.76	1.01
	SCB-4	0.56	9.3	6.6	9.1	8.9	0.71	0.96
Wang and Nie (1992)	CBI-1	0.74	15.2	12.6	16.3	16.3	0.83	1.07
	CBI-2	0.76	11.8	9	12	11.9	0.76	1.01
	CBI-3	0.77	7.9	5.8	8.2	8.1	0.73	1.03
	CBII-1	0.74	7.8	5.6	7.9	7.7	0.72	0.99
	CBII-2	0.72	7.6	5.1	7.2	7.1	0.67	0.93
	CBII-3	0.71	7.1	4.8	6.8	6.7	0.68	0.94
Li (1984)	B-1	0.55	4.3	3.5	4.7	4.6	0.81	1.07
	B-2	0.52	3.8	3.2	4.2	4.2	0.84	1.11
	B-3	0.58	4.3	3.5	4.9	4.8	0.81	1.12
	B-4	0.53	4.5	3.1	4.7	4.4	0.69	0.98
	B-6	0.56	4.3	3.3	4.4	4.4	0.77	1.02
	B-7	0.6	3.9	3.1	4.6	4.5	0.79	1.15
	BN-1	0.7	4.1	3.1	4.6	4.5	0.76	1.10
	BN-2	0.64	4.1	2.5	3.9	3.5	0.61	0.85
	BN-5	0.71	4.2	2.6	3.9	3.7	0.62	0.88
	BN-6	0.67	3.7	2.7	4.1	3.9	0.73	1.05
Chapman and Balakrishnan (1964)	A1	0.54	8.4	7.3	8.8	8.8	0.87	1.05
	A2	0.51	8.6	7.2	8.8	8.7	0.84	1.01
	A3	0.51	9.2	7.4	9.4	9.3	0.80	1.01
	A4	0.44	9	7.3	9.3	9.2	0.81	1.02
	A5	0.49	9.1	7.1	9.3	9.2	0.78	1.01
	A6	0.54	10	7.1	9.9	9.7	0.71	0.97
	B1	0.47	9.3	7.1	9.4	9.3	0.76	1.00
	C1	0.51	9	7.1	9.4	9.3	0.79	1.03
	D1	0.5	8.6	7.2	8.5	8.4	0.84	0.98
	E1	0.44	7.7	7.1	8.1	8	0.92	1.04
	F1	0.47	7.9	7.2	9.2	9.1	0.91	1.15
	U1	0.44	11.4	8.9	11.1	11.1	0.78	0.97
	U2	0.44	11.4	8.9	11.4	11.4	0.78	1.00
	U3	0.46	11.4	8.8	10.9	10.9	0.77	0.96
	U4	0.46	9.4	8.8	11.2	11.2	0.94	1.19
	Davies (1969)	A1	0.69	11.4	8.8	11.9	11.7	0.77
A2		0.68	6.4	5.6	7.9	7.7	0.88	1.20
A3		0.67	4.2	3.1	1.7	4.5	0.74	1.07

specimens SCB-1 and SCB-2 with specimens SCB-3 and SCB-4. The slip distribution of a typical specimen (SCB-3) across the section is shown in Fig. 10. The measured slip (strain discontinuity) between the steel and concrete is clearly observed.

The results from the formulas derived earlier are compared with the test results of the present study and also other available test measurements. Table 2 is for simply supported beams and Table 3 is for continuous beams.

In Table 2, P =actual loading; P_u =ultimate capacity; f_t =total measured deflection; f_e =calculated deflection using transformed section method without considering slip effect; f_{acu} =deflection calculated with formulas from Eqs. (28)–(30); and f_{app} =approximate deflection calculated using generalized formula Eq. (31). The specimens in this table include one-point concentrated load, two-point symmetric load, and uniform load. It can be seen that the transformed section method without considering slip effects underpredicts the deflection (column 8). In comparison, the formulas developed in this study predict very close results to the measurements (column 9).

For continuous beam in Table 3, the section rigidity near the supports ($0.15L$ of each side of the supports) is reduced by considering only the contribution from steel beam and reinforcement. The deflection is then calculated using the transformed section method. To consider the slip effects, this deflection is modified using $(1+\xi)$ and compared with measurements. Again, the procedure developed in the present study predicts close results to the measurement (column 8), while the transformed section method ignoring the slip effect underestimates the deflection (column 7).

Comparison with Design Specifications

While the slip effect on deflection has been recognized, it is not considered in the current AASHTO (1998) design specifications. In the AISC (1993) commentary, it is recommended that deflection and stress calculations of partially composite girders be based on the so-called effective moment of inertia and effective section modulus to account for slip effects as

Table 3. Comparison of Deflection for Continuous Beams

Specimen source	Specimen	P/P_u	f_t (mm)	f_e (mm)	f_{app} (mm)	f_e/f_t	f_{app}/f_t
Present study	CCB-1	0.72	5.5	4.2	6.2	0.76	1.13
	CCB-2	0.71	5.6	4.0	5.8	0.70	1.03
Newmark et al. (1951)	CCB-1	0.72	6.5	5.2	7.7	0.80	1.18
	CCB-2	0.72	6.6	4.7	7.0	0.71	1.06
	CCB-3	0.75	6.9	4.5	6.6	0.64	0.96
Zhu (1989)	L-3	0.7	5.8	4.1	5.6	0.70	0.96
	L-4	0.69	6.3	4.3	5.6	0.69	0.89
Ansourian (1981)	CTB1	0.75	9.1	7.1	9.0	0.78	0.99
	CTB2	0.71	8.1	6.3	7.4	0.77	0.91
	CTB3	0.72	7.9	6.0	7.5	0.76	0.95
	CTB4	0.71	8.8	6.1	7.7	0.69	0.88
	CTB5	0.71	6.6	4.8	6.5	0.73	0.99
	CTB6	0.72	5.9	4.8	6.2	0.82	1.05
Hope-Gill and Johnson (1976)	CB10	0.71	6.7	4.9	6.1	0.72	0.91
	CB11	0.73	14.5	7.8	13.3	0.54	0.92
	CB12	0.69	15.1	12.8	14.6	0.85	0.97

$$I_{eff} = I_s + \sqrt{\sum Q_n / C_f} (I_{tr} - I_s) \quad (45)$$

$$S_{eff} = S_s + \sqrt{\sum Q_n / C_f} (S_{tr} - S_s) \quad (46)$$

where I_{eff} =effective moment of inertia of composite section; I_s =moment of inertia of steel beam; $\sum Q_n$ =total shear strength of shear connectors provided; C_f =compression force in concrete slab of full composite section; I_{tr} =moment of inertia of trans-

formed section assuming full composite and uncracked section; S_{eff} =effective section modulus of composite section; S_s =section modulus of steel beam; and S_{tr} =section modulus of transformed section assuming full composite and uncracked section.

A realistic comparison between present study and the code specifications should be based on typical dimensions used in practice. For this reason, composite beams for different lengths are proportioned considering dead load and HS20 truckload. It is noted that though the beams were designed with the HS20 load,

Table 4. Dimensions and Parameters of Beams

Span length (m)	t_w (mm)	d_w (mm)	t_{top} (mm)	b_{top} (mm)	t_{bot} (mm)	b_{bot} (mm)	Full Composite ($k_p=1$)		50% Composite ($k_p=0.5$)		25% Composite ($k_p=0.25$)	
							αL	ξ	αL	ξ	αL	ξ
9.14	3.8	326.6	25.4	116.7	25.4	187.5	8.16	0.20	5.77	0.35	4.08	0.50
10.67	4.4	381.0	25.4	116.7	25.4	228.3	9.37	0.18	6.63	0.33	4.69	0.53
12.19	5.1	435.4	25.4	116.7	25.4	285.1	10.81	0.17	7.65	0.31	5.41	0.54
13.72	5.7	489.9	25.4	116.7	25.4	281.4	11.52	0.15	8.14	0.28	5.76	0.49
15.24	6.3	544.3	25.4	116.7	25.4	328.5	12.72	0.14	9.00	0.26	6.36	0.47
16.76	7.0	598.7	25.4	116.7	25.4	339.4	13.48	0.12	9.53	0.24	6.74	0.43
18.29	7.6	653.1	25.4	116.7	25.4	351.7	14.20	0.11	10.04	0.22	7.10	0.40
19.81	8.2	707.6	25.4	116.7	25.4	360.3	14.85	0.10	10.50	0.20	7.43	0.37
21.34	8.9	762.0	25.4	116.7	25.4	359.6	15.38	0.09	10.87	0.18	7.69	0.34
22.86	9.5	816.4	25.4	116.7	25.4	368.8	15.97	0.09	11.29	0.17	7.99	0.32
24.38	10.1	870.9	25.4	116.7	25.4	362.9	16.41	0.08	11.60	0.15	8.20	0.29
25.91	10.8	925.3	25.4	116.7	25.4	354.8	16.81	0.07	11.89	0.14	8.41	0.27
27.43	11.4	979.7	25.4	116.7	25.4	351.6	17.26	0.07	12.20	0.13	8.63	0.25
28.96	12.0	1034.1	25.4	116.7	25.4	347.2	17.68	0.06	12.50	0.12	8.84	0.23
30.48	12.7	1088.6	25.4	116.7	25.4	334.1	18.04	0.06	12.75	0.11	9.02	0.22
32.00	13.3	1143.0	25.4	116.7	25.4	319.7	18.39	0.05	13.00	0.11	9.19	0.20
33.53	13.9	1197.4	25.4	116.7	25.4	312.0	18.79	0.05	13.29	0.10	9.39	0.19
35.05	14.6	1251.9	25.4	116.7	25.4	295.5	19.14	0.05	13.53	0.09	9.57	0.18
36.58	15.2	1306.3	25.4	116.7	25.4	269.8	19.43	0.04	13.74	0.09	9.72	0.17
38.10	15.8	1360.7	25.4	116.7	25.4	251.5	19.79	0.04	13.99	0.08	9.89	0.15
39.62	16.5	1415.1	25.4	116.7	25.4	232.5	20.15	0.04	14.25	0.08	10.08	0.15
41.15	17.1	1469.6	25.4	116.7	25.4	213.1	20.52	0.04	14.51	0.07	10.26	0.14
42.67	17.7	1524.0	25.4	116.7	25.4	193.5	20.91	0.03	14.78	0.07	10.45	0.13
44.20	18.4	1578.4	25.4	116.7	25.4	164.0	21.26	0.03	15.03	0.06	10.63	0.12
45.72	19.0	1632.9	25.4	116.7	25.4	133.9	21.63	0.03	15.29	0.06	10.81	0.11

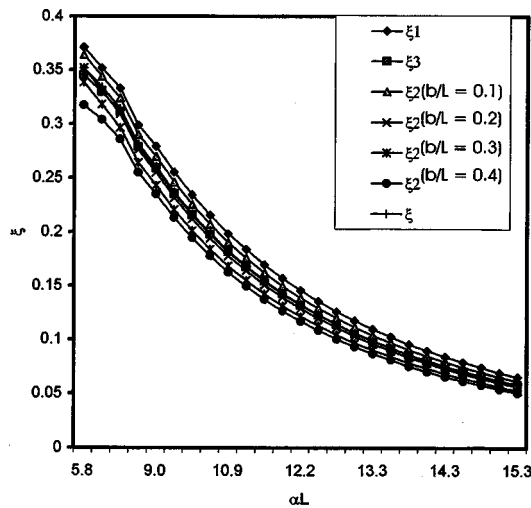


Fig. 11. Effect of load type on ξ ($k_p=0.5$)

discussions were conducted on the AISC specifications since AASHTO specifications do not consider the slip effects.

The following typical data are assumed in the calculations: concrete strength $f'_c=34.5$ MPa (5,000 psi), concrete elastic modulus $E_c=28,000$ MPa (4,030,000 psi), steel yield strength $f_y=345$ MPa (50,000 psi), steel elastic modulus $E_s=200,000$ MPa (29,000,000 psi), girder spacing $S_g=2,440$ mm (96 in.), slab thickness $t_s=200$ mm (8 in.), the steel web depth to span length (d_w/L)=1/28; steel top and bottom flange thicknesses t_{top} and $t_{bot}=25$ mm (1 in.); and web thickness and top flange width are

calculated based on the slenderness requirement of the specifications. Finally, the bottom flange width is calculated by equating the member capacity to the load effect, i.e., $\phi M_n=M_u$.

The proportioned beam dimensions are summarized in Table 4 with span length from 9.1 to 45.7 m. According to Nie and Shen (1997), the effect of slip on ultimate strength of composite beam can be ignored. The strength reduction due to the effect of slip is thus not considered in the present strength design. However, for the stiffness calculation, different degree of composite action is considered and indicated by a parameter $k_p=\Sigma Q_n/C_f$. The k_p value of 1.0, 0.5, and 0.25 represents full composite action, 50% composite action, and 25% composite action, respectively. The shear stud pitch p is calculated from the parameter k_p and p_f as

$$p = \frac{1}{k_p} p_f = \frac{1}{k_p} \frac{0.5Ln_s Q_n}{C_f} \quad (47)$$

where n_s =number of shear studs per row across the flange; and p_f =stud pitch required for full composite action.

It can be seen from Table 4 that αL is at least 4.0 even in the extreme case with $k_p=0.25$, which verifies the assumption of $e^{-\alpha L} \cong 0$. The comparison of the generalized ξ and their original form for different load types is plotted in Fig. 11. It can be seen that all the ξ values fall within a narrow band with the generalized one approximately in the middle, meaning the generalization should not result in a significant error for different load types. This, along with the reason that actual beams carry different type of loads, justifies the generalization of ξ made earlier.

In Table 5, the effective modulus and moment of inertia from formulas Eqs. (32) and (44), normalized by their values based on

Table 5. Comparison between Present Study and American Institute of Steel Construction Specification

Span length (m)	Full Composite ($k_p=1$)				50% Composite ($k_p=0.5$)				25% Composite ($k_p=0.25$)			
	Present S_{eff}/S_{tr}	AISC S_{eff}/S_{tr}	Present I_{eff}/I_{tr}	AISC I_{eff}/I_{tr}	Present S_{eff}/S_{tr}	AISC S_{eff}/S_{tr}	Present I_{eff}/I_{tr}	AISC I_{eff}/I_{tr}	Present S_{eff}/S_{tr}	AISC S_{eff}/S_{tr}	Present I_{eff}/I_{tr}	AISC I_{eff}/I_{tr}
9.14	0.98	1.00	0.83	1.00	0.97	0.87	0.74	0.76	0.96	0.77	0.67	0.59
10.67	0.98	1.00	0.84	1.00	0.97	0.88	0.75	0.76	0.96	0.79	0.65	0.59
12.19	0.99	1.00	0.86	1.00	0.97	0.89	0.76	0.76	0.96	0.82	0.65	0.59
13.72	0.99	1.00	0.87	1.00	0.97	0.90	0.78	0.77	0.96	0.83	0.67	0.60
15.24	0.99	1.00	0.88	1.00	0.98	0.91	0.79	0.77	0.96	0.84	0.68	0.60
16.76	0.99	1.00	0.89	1.00	0.98	0.91	0.81	0.77	0.96	0.84	0.70	0.61
18.29	0.99	1.00	0.90	1.00	0.98	0.91	0.82	0.77	0.96	0.85	0.71	0.61
19.81	0.99	1.00	0.91	1.00	0.98	0.91	0.83	0.77	0.96	0.85	0.73	0.61
21.34	0.99	1.00	0.91	1.00	0.98	0.91	0.85	0.78	0.96	0.85	0.75	0.62
22.86	0.99	1.00	0.92	1.00	0.98	0.91	0.86	0.78	0.96	0.85	0.76	0.62
24.38	0.99	1.00	0.93	1.00	0.98	0.91	0.87	0.78	0.96	0.85	0.77	0.62
25.91	0.99	1.00	0.93	1.00	0.98	0.91	0.87	0.78	0.95	0.85	0.79	0.63
27.43	0.99	1.00	0.94	1.00	0.98	0.91	0.88	0.78	0.95	0.84	0.80	0.63
28.96	0.99	1.00	0.94	1.00	0.97	0.91	0.89	0.79	0.95	0.84	0.81	0.63
30.48	0.99	1.00	0.94	1.00	0.97	0.91	0.90	0.79	0.95	0.84	0.82	0.64
32.00	0.99	1.00	0.95	1.00	0.97	0.90	0.90	0.79	0.95	0.83	0.83	0.64
33.53	0.99	1.00	0.95	1.00	0.97	0.90	0.91	0.79	0.95	0.83	0.84	0.65
35.05	0.99	1.00	0.95	1.00	0.97	0.90	0.92	0.79	0.95	0.83	0.85	0.65
36.58	0.99	1.00	0.96	1.00	0.97	0.90	0.92	0.80	0.95	0.82	0.86	0.65
38.10	0.99	1.00	0.96	1.00	0.97	0.89	0.93	0.80	0.95	0.82	0.87	0.66
39.62	0.99	1.00	0.96	1.00	0.97	0.89	0.93	0.80	0.95	0.81	0.87	0.66
41.15	0.99	1.00	0.97	1.00	0.97	0.89	0.93	0.80	0.95	0.81	0.88	0.66
42.67	0.99	1.00	0.97	1.00	0.97	0.89	0.94	0.80	0.95	0.81	0.89	0.66
44.20	0.99	1.00	0.97	1.00	0.97	0.88	0.94	0.80	0.95	0.80	0.89	0.67
45.72	0.99	1.00	0.97	1.00	0.97	0.88	0.94	0.81	0.95	0.79	0.90	0.67

transformed section, are compared with that from Eqs. (45) and (46), the AISC formulas. It can be seen that even for the full composite section, the present study predicts a reduction up to 2% (column 2) for section modulus and a reduction ranging from 3% to 17% (column 4) for moment of inertia. In comparison, the AISC code specifications do not consider the reduction due to slip (columns 3 and 5), meaning that the AISC is on the unconservative side for the full composite section.

For 50% composite, the present study predicts up to 3% (column 6) and 26% (column 8) reduction in section modulus and moment of inertia, respectively, compared with up to 13% (column 7) and 24% (column 9) for AISC specifications. For 25% composite, the present study predicts up to 5% (column 10) and 33% (column 12) reduction in section modulus and moment of inertia, respectively, compared with up to 23% (column 11) and 41% (column 13) for AISC specifications. Generally, the AISC specifications are more conservative than the present study for the partial composite section.

Summary and Conclusions

The equivalent rigidity of beams considering three different loading types was derived based on equilibrium and curvature compatibility, on which a general formula to account for slip effects was developed. The results were then compared with available test results for both simply supported and continuous beams. Including slip effects has significantly improved the accuracy of deflection predictions. The test results justify the assumptions made in the present study.

According to the present study for typical beams used in practice (for span ranging from 9.1 to 45.7 m), shear slip between the interface of steel and concrete in partial composite beam has a considerable contribution to the beam deformation. Even for full composite beams, slip effects may result in stiffness reduction up to 17% for short span beams. In general, the slip effect on section modulus is less than that on moment of inertia.

The slip effects are ignored in many design specifications that use transformed section method. In the commentary of AISC specifications (AISC 1993), stress and deflection calculations of partially composite girders are based on effective section modulus and effective moment of inertia to account for slip, while ignoring slip effects in full composite sections. Therefore, for full composite sections, the predicted effective section modulus and moment of inertia with AISC design specifications are unconservative compared with the present study. For partial composite section, the AISC predictions are more conservative than the present study.

Deflection is a control parameter in modern bridge designs that use high strength steel and high strength concrete. While underestimated deflection may result in serviceability problem, an overestimated deflection would result in a rejection of a design, which would have adverse financial effects on the project. Therefore, accurate prediction of deflection in a reasonable effort becomes increasingly important in modern bridge design.

Acknowledgments

The research of the first writer was supported by the Chinese National Funds for Outstanding Young Investigators. The help from the staff at the Research Institute of Structural Engineering, Tsinghua Univ., in carrying out the experimental program is very

much appreciated. The second writer was partially supported by the Faculty Development Award, Kansas State Univ. The very constructive comments from the reviewers are very much appreciated.

Notation

The following symbols are used in this paper:

- A_c = area of concrete;
- A_{ft} = area of top flange;
- A_s = area of steel;
- A_w = area of web;
- $A_0 = (A_s A_c) / (n A_s + A_c)$;
- $A_1 = A_0 / (I_0 + A_0 d_c^2)$;
- b = distance between loading point and mid span;
- C = compression in concrete;
- C_f = compression force in concrete slab of full composite section;
- $d_c = y_{cb} + y_{st}$;
- d_w = steel web depth;
- E_c = elastic modulus of concrete;
- E_s = elastic modulus of steel;
- $EI = E_s (I_0 + A_0 d_c^2) = E_s A_0 / A_1$ = rigidity of transformed section;
- f'_c = concrete strength;
- f_{acc} = deflection calculated with formulas from Eqs. (28) to (30);
- f_{app} = approximate deflection calculated using generalized formula Eq. (31);
- f_e = deflection using transformed section method without considering slip;
- f_t = total measured deflection;
- f_y = steel yield strength;
- h = depth of entire section;
- h_c = depth of concrete;
- h_s = depth of steel;
- I_c = moment inertia of concrete;
- I_{eff} = effective moment of inertia of composite section;
- I_s = moment of inertia of steel beam;
- I_{tr} = moment of inertia of transformed section;
- $I_0 = I_c / n + I_s$;
- K = shear stiffness of shear stud;
- k_p = parameter for degree of composite action;
- M = internal moment without slip;
- M_c = moment carried by concrete;
- M_p = internal moment including slip;
- M_{py} = first yield moment considering slip;
- M_s = moment carried by steel;
- M_y = first yield moment without slip;
- $n = E_s / E_c$;
- n_s = number of shear studs per row across flange;
- P = total load at mid span;
- P_u = ultimate capacity;
- p = longitudinal spacing (pitch) of shear studs;
- p_f = shear stud spacing for full composite action;
- S = slip between steel and concrete;
- S_{eff} = effective section modulus of composite section;
- S_g = girder spacing;
- S_s = section modulus of steel beam;
- S_{tr} = section modulus of transformed section;
- T = tension in steel;
- t_{bot} = thickness of bottom flange;

t_s = slab thickness;
 t_{top} = thicknesses of top flange;
 V_c = shear force carried by concrete;
 V_s = shear force carried by steel;
 y_{cb} = distance from bottom of concrete to its neutral axis;
 y_{st} = distance from top of steel to its neutral axis;
 ∇M = moment variation in section due to slip;
 $\alpha^2 = K/(A_1 E_s I_0 p)$;
 $\beta = A_1 d_c p / K$;
 ϵ_{cb} = strain at bottom of concrete;
 ϵ_{cs} = slip strain at bottom of concrete;
 ϵ_{ss} = slip strain at top of steel;
 ϵ_{st} = strain at top of steel;
 $\eta = 24EI\beta/(L^2 h)$;
 ξ = parameter for slip effect;
 σ = normal stress between steel and concrete interface;
 ΣQ_n = total shear strength of shear connectors provided; and
 τ = shear stress.

References

- American Association of State Highway and Transportation Officials (AASHTO). (1998). "LRFD bridge design specifications." Washington, D.C.
- American Institute of Steel Construction (AISC). (1993). "Load and resistance factor design." Chicago.
- Ansourian, P. (1981). "Experiments on continuous composite beams." *Proc., Inst. Civ. Eng.*, 71(2), 25–51.
- Chapman, J. C., and Balakrishnan, S. (1964). "Experiments on composite beams." *Struct. Eng.*, 42(11), 369–383.
- Davies, C. (1969). "Test on half-scale steel-concrete composite beams with welded stud connectors." *Struct. Eng.*, 47(1), 29–40.
- Dezi, L., Gara, F., Leoni, G., and Tarantino, A. M. (2001). "Time-dependent analysis of shear-lag effect in composite beams." *J. Eng. Mech.*, 127(1), 71–79.
- Grant, J. A., Fisher, J. W., and Slutter, R. G. (1977). "Composite beams with formed steel deck." *AISC Eng. J.*, 12(1), 24–43.
- Hope-Gill, M. C., and Johnson, R. P. (1976). "Test on three-span continuous composite beams." *Proc., Inst. Civ. Eng.*, 367–381.
- Johnson, R. P. (1975). *Composite structures of steel and concrete*, Granada Limited.
- Li, T. (1984). "Experiments and performance analysis of simply supported steel-concrete composite beam under short-term loading." Master Thesis, Zhengzhou Institute of Technology, Zhengzhou, China (in Chinese).
- Manfredi, G., Fabbrocino, G., and Cosenza, E. (1999). "Modeling of steel-concrete composite beams under negative bending." *J. Eng. Mech.*, 125(6), 654–662.
- McGarraugh, J. B., and Baldwin, J. W. (1971). "Lightweight concrete-on-steel composite beams." *AISC Eng. J.*, 8(3).
- Newmark, N. M., Siess, C. P., and Viest, I. M. (1951). "Test and analysis of composite beams with incomplete interaction." *Exp. Stress Anal.*, 9(1), 75–92.
- Nie, J. G., and Shen, J. M. (1997). "Slip effect on strength of composite steel-concrete beams." *China Civil Eng. J.*, China Civil Engineering Society, 30(1), 31–36 (in Chinese).
- Sebastian, W. M., and McConnel, R. E. (2000). "Nonlinear FE analysis of steel-concrete composite structures." *J. Struct. Eng.*, 126(6), 662–674.
- Wang, Q. H., and Nie, J. G. (1992). "Steel-concrete composite beam using regular precast reinforced slab as compression flange." *J. Industrial Building*, 22(2), 6–9 (in Chinese).
- Zhu, P. R. (1989). *Principles of steel-concrete composite beams*, China Building Industrial Press, Beijing (in Chinese).